

ITP-SB-95-60
LBL-38282

Charm and Bottom Quark Production Cross Sections Near Threshold

J. SMITH

*Institute for Theoretical Physics,
State University of New York at Stony Brook,
Stony Brook, NY 11794-3840*

R. VOGT¹

*Nuclear Science Division,
Lawrence Berkeley National Laboratory,
Berkeley, California 94720
and
Physics Department,
University of California at Davis,
Davis, California 95616 USA*

April 1996

Abstract

The cross sections for charm and bottom quark production in the threshold region are discussed. We consider the effects of an all order resummation of initial state soft-plus-virtual gluon radiation on the total cross sections compared to the order α_s^3 results.

¹This work was supported in part by the Director, Office of Energy Research, Division of Nuclear Physics of the Office of High Energy and Nuclear Physics of the U. S. Department of Energy under Contract Number DE-AC03-76SF0098.

Heavy quark production has long been a topic of interest, both experimentally and theoretically. Early measurements of the total $c\bar{c}$ production cross section at $\sqrt{S} \leq 63$ GeV suggested that the calculated Born (LO) cross section underpredicted the data by a factor of two to three [1, 2], known as the K factor after a similar situation in Drell-Yan production. In general,

$$K_{\text{exp}} = \frac{\sigma_{\text{data}}(AB \rightarrow Q\bar{Q})}{\sigma_{\text{theory}}(AB \rightarrow Q\bar{Q})}, \quad (1)$$

where Q is the heavy quark (c , b , or t) and σ_{theory} is calculated to fixed order in the running coupling constant α_s . The next-to-leading order (NLO) corrections to the Born cross section have been calculated [3, 4, 5] and an analogous theoretical K factor is defined by the ratio of the NLO to the LO cross sections,

$$K_{\text{th}} = \frac{\sigma^{\text{NLO}}(AB \rightarrow Q\bar{Q})}{\sigma^{(0)}(AB \rightarrow Q\bar{Q})}, \quad (2)$$

where $\sigma^{(0)}$ is the LO cross section and σ^{NLO} is the sum of the LO and the exact $\mathcal{O}(\alpha_s)$ correction, $\sigma^{\text{NLO}} = \sigma^{(0)} + \sigma^{(1)}|_{\text{exact}}$.

The heavy quark production cross section is calculated in QCD by assuming the validity of the factorization theorem [6] and expanding the contributions to the amplitude in powers of the coupling constant $\alpha_s(\mu^2)$. The hadronic production cross section at hadronic center of mass energy \sqrt{S} and to order $\alpha_s^{(k)}$ is

$$\sigma^{(k)}(S, m^2) = \sum_{ij} \int_{\frac{4m^2}{S}}^1 d\tau \int_{\tau}^1 \frac{dx}{x} f_i^{h_1}(x, \mu^2) f_j^{h_2}\left(\frac{\tau}{x}, \mu^2\right) \sigma_{ij}^{(k)}(\tau S, m^2, \mu^2), \quad (3)$$

where $f_i^h(x, \mu^2)$ are the scale-dependent parton densities of hadron h evaluated at the scale μ^2 and $\sigma_{ij}^{(k)}$ is the k^{th} order partonic cross section for $ij \rightarrow Q\bar{Q}X$. The total cross section up to order k is $\sum_k \sigma^{(k)}(S, m^2)$. The numerical results for “lighter” heavy quark production depend on the choice of the parton densities, involving the mass factorization scale μ_F , the running coupling constant, evaluated at the renormalization scale μ_R , and the heavy quark mass m . Usually the renormalization and factorization scales are assumed to be equal, $\mu_R = \mu_F = \mu$. All these factors influence both K_{exp} and K_{th} .

At LO the cross section is very sensitive to the mass and scale parameters. However even including the NLO corrections cannot completely fix the cross

section. The sensitivity to even higher terms in the QCD expansion is often demonstrated by varying μ between $m/2$ and $2m$. This may not be very meaningful, especially for charm, since a variation of an order of magnitude or more is observed. It is therefore not clear that the next-to-next-to-leading order (NNLO) corrections are not at least as large as the NLO corrections, particularly when $m \ll \sqrt{S}$. Given these facts, it is impossible to make more precise predictions in the absence of a NNLO calculation.

Recently two groups have attempted to use the NLO calculations to make more definitive statements about charm production [7, 8, 9]. The NLO calculations were compared to charm production data in pp and π^-p interactions [1, 2, 10, 11]. In the first approach [7, 8], the data were used to fix m_c and μ by requiring $K_{\text{exp}}^{\text{NLO}} \sim 1$ in an attempt to place bounds on charm production at nuclear colliders. Two recent parton densities², MRS D—' [13, 14] and GRV HO [15, 16] were used in the comparison. Reasonable agreement was found for $m_c = 1.2 \text{ GeV}/c^2$, $\mu = 2m_c$ with MRS D—' [13, 14] and for $m_c = 1.3 \text{ GeV}/c^2$, $\mu = m_c$ with GRV HO [15, 16] although both results tend to underestimate the total $c\bar{c}$ production cross section, $\sigma_{c\bar{c}}^{\text{tot}}$, with $K_{\text{exp}}^{\text{NLO}} \sim 1.1 - 2$. In the range of the parameter space defined by m_c , μ_R and μ_F , $K_{\text{exp}}^{\text{NLO}}$ can be reduced to unity. However, it is questionable if the mass and scale values needed for $K_{\text{exp}}^{\text{NLO}} \sim 1$ are consistent with a perturbative treatment and with the defined limits of the parton density distributions. In another approach, calculations using a charm mass of $m_c = 1.5 \text{ GeV}/c^2$ produced results compatible with the data although with some essential caveats: μ_F and μ_R were varied independently and out-of-date parton distributions fit with several values of Λ_{QCD} were used [9]. Decreasing μ_R with respect to μ_F and increasing Λ_{QCD} result in significantly larger cross sections for a given m_c . Additionally, different parton densities were used in the calculations of $\sigma_{Q\bar{Q}}^{\text{tot}}$ and high energy b production. Neither approach is fully satisfactory: either an uncomfortably small charm quark mass is needed or the parameters used to describe low energy production are incompatible with those used at collider energies.

Although a complete calculation of still higher order terms is not possible for all values of S and m , improvements may be made in specific kinematical regions. Investigations have shown that near threshold there can be large

²All available parton densities for the nucleon and the pion can be found in PDFLIB [12].

logarithms in the perturbative expansion which must be resummed to make more reliable theoretical predictions. These large logarithms arise from an imperfect cancellation of the soft-plus-virtual (S+V) terms. In [17] an approximation was given for the S+V gluon contributions and the analogy with the Drell-Yan process, studied in [18, 19], was exploited to resum these to all orders of perturbation theory. The same resummation procedure was also applied to $\sigma_{t\bar{t}}^{\text{tot}}$ and inclusive top quark distributions in $p\bar{p}$ collisions at the Fermilab Tevatron [17, 20, 21]. For top production in $p\bar{p}$ collisions, $q\bar{q}$ annihilation is the dominant process, fortunate since the exponentiation of the S+V terms [17] is better understood because the simple color structure has a close correspondence to the Drell-Yan studies [18, 19].

The resummation of the leading S+V terms [17] modifies eq. (3) so that

$$\sigma^{\text{res}}(S, m^2) = \sum_{ij} \int_{\tau_0}^1 d\tau \int_{\tau}^1 \frac{dx}{x} f_i^{h_1}(x, \mu^2) f_j^{h_2}\left(\frac{\tau}{x}, \mu^2\right) \sigma_{ij}^{\text{res}}(\tau S, m^2), \quad (4)$$

where

$$\sigma_{ij}^{\text{res}}(\tau S, m^2) = - \int_{s_0}^{s-2ms^{1/2}} ds_4 f\left(\frac{s_4}{m^2}, \frac{m^2}{\mu^2}\right) \frac{d\bar{\sigma}_{ij}^{(0)}(s, s_4, m^2)}{ds_4}. \quad (5)$$

The integration variable s_4 , an invariant which measures the four-momentum carried away by the final-state gluon in the process $i(k_1) + j(k_2) \rightarrow Q(p_1) + \bar{Q}(p_2) + g(k_3)$, is defined as $s_4 = s + t + u - 2m^2$ where $s = (k_1 + k_2)^2$, $t = (k_1 - p_1)^2$, and $u = (k_1 - p_2)^2$. The cross section $\bar{\sigma}_{ij}^{(0)}(s, s_4, m^2)$ is the angle-averaged Born cross section and $\bar{\sigma}_{ij}^{(0)}(s, 0, m^2) \equiv \sigma_{ij}^{(0)}(s, m^2)$. The function $f(s_4/m^2, m^2/\mu^2)$ is

$$f\left(\frac{s_4}{m^2}, \frac{m^2}{\mu^2}\right) = \exp\left[A \frac{C_{ij}}{\pi} \bar{\alpha}_s\left(\frac{s_4}{m^2}, m^2\right) \ln^2 \frac{s_4}{m^2}\right] \frac{[s_4/m^2]^\eta}{\Gamma(1+\eta)} \exp(-\eta\gamma_E), \quad (6)$$

where γ_E is the Euler constant, $\eta = (8C_{ij}/\beta_0) \ln(1 + (\beta_0\alpha_s(\mu^2)/4\pi) \ln(m^2/\mu^2))$, $\beta_0 = 11 - 2n_f/3$ for SU(3), and A and $\bar{\alpha}_s$ are scheme dependent. In *e.g.* the $\overline{\text{MS}}$ scheme, $A = 2$ and $\bar{\alpha}_s((s_4/m^2), m^2) = \alpha_s(s_4^{2/3} m^{2/3})$. The integral over s_4 has been split into two parts and the integral over the region $0 < s_4 < s_0$, where the running coupling becomes infinite as $s_4 \rightarrow 0$, is assumed to be negligible. This condition is satisfied if $s_0/m^2 \ll 1$. The lower limit on the τ integral is

$$\tau_0 = \frac{[m + (m^2 + s_0)^{1/2}]^2}{S}, \quad (7)$$

where $s_0 = m^2(\mu_0^2/\mu^2)^{3/2}$ in the $\overline{\text{MS}}$ scheme and $s_0 = m^2(\mu_0^2/\mu^2)$ in the DIS scheme. The cutoff parameter μ_0 , introduced in [19, 22], monitors the sensitivity of the cross section to nonperturbative higher-twist effects. If σ_{ij}^{res} is strongly dependent on μ_0 , a precise determination of the cross section requires full knowledge of the nonperturbative contributions. As may be expected, the resummed corrections diverge for small μ_0 [17].

The resummation technique has recently been applied to $b\bar{b}$ production in pp interactions [23] at HERA-B ($\sqrt{S} = 39.2$ GeV) [24, 25] where gluon fusion is the dominant channel. The gg channel is not as amenable to the resummation technique because each of the Born diagrams has a different color structure³. Therefore it is important to test the model in a regime where data already exists. Charm and bottom production data from pp and π^-p interactions are available at energies where the resummation technique can be applied. An advantage of the pion beam is the relative importance of the $q\bar{q}$ channel in $c\bar{c}$ and $b\bar{b}$ production. However charm production must be treated with some care. The data is available for $\sqrt{S} \geq 15$ GeV where the expansion parameter, $\alpha_s(m^2) \ln(\sqrt{S}/m)$, is not small. However, if the model is reliable for charm production, a better understanding of $c\bar{c}$ production at the lower fixed-target energies may be reached.

Since we wish to compare our results with data taken using both pion and proton beams, we are rather constrained in our choice of parton distribution functions. The only consistent NLO evaluation of the pion and proton parton densities has been done by GRV [15, 16]. Because the GRV HO parameterization is in the $\overline{\text{MS}}$ scheme, we are forced to use this scheme for both the $q\bar{q}$ and gg channels. Thus the value of μ_0 needed for stability of the resummed result in the $q\bar{q}$ channel is likely to be larger than found previously [17, 20, 21, 23]. Our results for the exact, approximate, and resummed hadronic cross sections will be calculated using these distributions along with the two-loop uncorrected running coupling constant⁴. This set has the additional advantage of a rather small initial scale so that we can use $\mu = m_c$ in our calculations. We therefore take $m_c = \mu = 1.5$ GeV/ c^2 and $m_b = \mu = 4.75$ GeV/ c^2 , along with the GRV HO parton densities and the $\overline{\text{MS}}$ scheme for our principle results. We will also show the range of resummed

³Quark-gluon scattering, producing a final state quark or antiquark, cannot be resummed by this method since there is no equivalent Born term.

⁴The difference between the uncorrected running coupling constant and the corrected value given by PDFLIB [12] is small, $\approx 3\text{-}4\%$.

cross sections by varying all these parameters, including the parton densities. In Table 1 we give the value of Λ_{nf} , μ and α_s for each value of m and set of parton densities we consider. The choice of these particular parameters will be explained later.

We first review the NLO contributions to $c\bar{c}$ and $b\bar{b}$ production [3, 4, 5]. In Fig. 1 we show the relative contributions of the gg , $q\bar{q}$, and the $(q + \bar{q})g$ channels as functions of \sqrt{S} for $c\bar{c}$ and $b\bar{b}$ production in π^-p and pp interactions. It is clear that $c\bar{c}$ production is almost entirely dominated by gluon fusion. In π^-p interactions at $\sqrt{S} \approx 10$ GeV the gg channel accounts for half the cross section. However, the gluon contribution increases to more than 80% soon afterward and the gg channel in pp production is always $\approx 90\%$ of the total cross section. Note that the quark-gluon scattering contribution is negative at low energies but changes sign at $\sqrt{S} \approx 40$ GeV. The $q\bar{q}$ annihilation contribution is larger for $b\bar{b}$ production, particularly for π^-p interactions where this channel is dominant until $\sqrt{S} \approx 40$ GeV. This situation is similar to top production in $p\bar{p}$ collisions at the Fermilab Tevatron. The pp production cross section is again dominated by gluon fusion, between 70-80% of the total, somewhat less than the gg contribution to $c\bar{c}$ production at the same energies. Quark-gluon scattering always gives a negative contribution to the total $b\bar{b}$ cross section for the energies considered. Note that although we show the $b\bar{b}$ results for $\sqrt{S} = 10$ GeV, the calculation is most reliable for $\sqrt{S} \geq 20$ GeV.

The resulting theoretical K factors for the total cross sections reflect the uncertainties in the dominant channels. Thus for $c\bar{c}$ production, $K_{\text{th}} > 2$, near the gluon K_{th} , over a large energy range. Likewise, K_{th} is smaller for $\pi^-p \rightarrow b\bar{b}$ interactions because of the dominant $q\bar{q}$ contribution for $\sqrt{S} \leq 40$ GeV. The $q\bar{q}$ channel is most amenable to resummation because even above threshold the NLO corrections are small. Above threshold in the gg channel, the NLO contribution increases as a function of $\sqrt{S}/2m$ and becomes constant at high energies while the Born contribution decreases to zero, resulting in large corrections. In $b\bar{b}$ production K_{th} is large for both channels near threshold.

In Fig. 2 we examine the μ_0 dependence of the resummed cross section using our parameters for $c\bar{c}$ production at $\sqrt{S} = 15$ GeV and $b\bar{b}$ production at $\sqrt{S} = 30$ GeV. We also show, for comparison, the μ_0 dependence of the

approximate NNLO cross section,

$$\sigma^{\text{app}} \equiv \sigma^{(0)} + \sigma^{(1)}|_{\text{app}} + \sigma^{(2)}|_{\text{app}}, \quad (8)$$

where we have imposed the same s_4 ($s_4 > s_0$) phase space cut on σ^{app} as on the resummed cross section. Here $\sigma^{(1)}|_{\text{app}}$ and $\sigma^{(2)}|_{\text{app}}$ denote the approximate first and second order corrections, respectively, where only soft gluon contributions are taken into account. Note that the phase space cut is also applied to $\sigma^{(0)}$. The effect of the resummation is apparent in the difference between the curves. At small μ_0 , σ^{res} diverges, signalling the onset of non-perturbative physics. In a study of $b\bar{b}$ production at HERA-B [23], μ_0 was chosen so that the resummed cross section remains somewhat larger than σ^{app} in each channel, namely $\mu_0 = 0.13m$ in the $q\bar{q}$ channel with the MRS D-’ DIS distributions and $\mu_0 = 0.36m$ in the gg channel, quite similar to earlier choices for top quark production [20]⁵. We choose the same ratios [23] for the gg channel, so that $\mu_0 \approx 0.35m$. Reasonable convergence is seen for this value, even for $c\bar{c}$ production, although σ^{res} remains larger than σ^{app} for all values of μ_0/m shown. Even though our calculation is in the $\overline{\text{MS}}$ scheme, convergence is found for $\mu_0 \approx 0.15m$ in the $q\bar{q}$ channel, not significantly larger than that of the DIS scheme.

In Fig. 3 we plot the resummed cross section with our chosen values of μ_0 as a function of center of mass energy for $c\bar{c}$ and $b\bar{b}$ production at fixed-target energies. Since the exact $O(\alpha_s^3)$ results are known, we also show the perturbation theory improved cross sections defined by

$$\sigma^{\text{imp}} = \sigma^{\text{res}} + \sigma^{(1)}|_{\text{exact}} - \sigma^{(1)}|_{\text{app}}, \quad (9)$$

to exploit the fact that $\sigma^{(1)}|_{\text{exact}}$ is known and $\sigma^{(1)}|_{\text{app}}$ is included in σ^{res} . The difference between σ^{res} and σ^{imp} is larger in pp production, presumably because the $q\bar{q}$ approximation of $\sigma^{(1)}|_{\text{exact}}$ is better than the gg approximation. We also show the NLO cross section calculated with the same mass and scale factors as σ^{res} and σ^{imp} . The resummed and NNLO approximate cross sections were calculated with the cut $s_4 > s_0$ while no cut was imposed on the NLO result. We can expect the resummation technique to work well in both the $q\bar{q}$ and gg channels when $m/\sqrt{S} \leq 0.1$ because the NLO contribution

⁵An application of principal value resummation leads to very similar results for the top quark production cross section [26].

is small compared to the LO term and the perturbation series should then converge. The effect of resummation is large for $c\bar{c}$ production, increasing the cross section by a factor of five or more relative to the NLO result. The agreement with the $c\bar{c}$ data from π^-p [1, 2, 11] and pp [1, 2, 10] interactions is improved by the resummation. The agreement with the existing $b\bar{b}$ data from π^-p [27] interactions is also somewhat improved. In general, we see that $K_{\text{exp}}^{\text{res}}$ is much smaller than $K_{\text{exp}}^{\text{NLO}}$ for the same m , μ , and parton densities. However, for charm quark production, the technique is questionable above $\sqrt{S} = 15$ GeV. The expansion parameter is proportional to $\alpha_s(m^2) \ln(\sqrt{S}/m)$ so that when $10 \leq \sqrt{S} \leq 30$ GeV, $0.53 \leq \alpha_s(m_c^2) \ln(\sqrt{S}/m_c) \leq 0.83$ where $\alpha_s(m_c^2)$ for the GRV HO distributions is found in Table 1. We have shown the $c\bar{c}$ results up to $\sqrt{S} = 30$ GeV even though the perturbative expansion no longer converges and resummation fails in the gg channel. This can be clearly seen in the faster increase of σ^{res} and σ^{imp} with energy compared to σ^{NLO} for $\sqrt{S} > 20$ GeV in Fig. 3(a).

We have also checked the resummation technique for a range of heavy quark masses, scales, and parton densities. The variation in the results is indicated by the dotted curves in Fig. 3. Outside the range indicated by the dotted curves, the resummation technique becomes questionable, particularly for the bound given by the upper dotted curve. When examining $b\bar{b}$ production, we studied the mass and scale dependence over the range $4.5 \leq m_b \leq 5$ GeV/ c^2 and $m_b/2 \leq \mu \leq 2m_b$. The $b\bar{b}$ results are more stable with respect to the variation, as indicated by the narrower bands in Fig. 3(c) and (d). We varied the charm quark mass between 1.3 and 1.8 GeV/ c^2 . Since the charm quark mass is relatively light, we study the scale dependence indirectly. Note also that the resummation technique cannot be applied to scales where $\mu < m_c$ because a perturbative treatment is uncertain for mass scales of ~ 1 GeV/ c^2 .

We also studied the parton density dependence so that along with the GRV HO distributions we also used the GRV LO and the MRS D- $'$ proton distributions. Since the resummed cross section depends on $\sigma^{(0)}$, it is instructive to compare the results using LO parton densities with the one-loop coupling constant to the NLO parton densities with the two-loop running coupling. We also used the MRS D- $'$ [14] and SMRS P2 [13] pion densities for $\overline{\text{MS}}$ π^-p production. The low x behavior of the SMRS densities is different than the MRS D- $'$ densities. Presumably adjusting the behavior of the SMRS low x region to match that of the proton densities would shift

the large x contribution in the threshold region. Additionally, because Λ_{QCD} is different for the two sets we use the value obtained in the proton fit. Finally for the MRS distributions the initial scale is larger than m_c , $Q_0^2 = 5 \text{ (GeV}/c)^2$. Therefore when we calculate $c\bar{c}$ production with these densities, we take $\mu = 2m_c$ instead of a full scale variation while we use $\mu = m_c$ for the GRV distributions.

The larger value of α_s at one-loop both increases the cross section with the GRV LO distributions as well as making the convergence of the perturbation series slower for both $c\bar{c}$ and $b\bar{b}$ production. In fact, since $\alpha_s \sim 0.38$ at one-loop for $m_c = 1.5 \text{ GeV}/c^2$, the resummation technique appears to fail for the gg case even at this relatively low energy, $\sqrt{S} = 15 \text{ GeV}$. In general, larger values of μ makes the convergence of the perturbation series unreliable. When $\mu = 2m$, s_0 is reduced by a factor of four, resulting in a large $\bar{\alpha}_s$ in the exponent in eq. (6). Thus a much larger μ_0 is needed for convergence, $\mu_0 \sim 0.5m_c$ in the $q\bar{q}$ channel and $\mu_0 \sim 0.7m_c$ in the gg channel with the MRS D- $'$ distributions, much too large to be compatible with the earlier results [17, 20, 21, 23]⁶. We also compared the $\overline{\text{MS}}$ and DIS schemes for the $q\bar{q}$ channel when appropriate. For both the GRV LO and MRS D- $'$ DIS distributions (applied to pp production only since the SMRS pion distributions are only available in the $\overline{\text{MS}}$ scheme) we found convergence for a smaller value of μ_0 and a correspondingly reduced $\sigma_{q\bar{q}}^{\text{res}}$, as expected. However, since the gluon can only be calculated in the $\overline{\text{MS}}$ scheme for consistency we give our results in the $\overline{\text{MS}}$ scheme for both channels.

The extremes we found that still allowed the cross section to be resummed are shown in the dotted curves of Fig. 3. Note that these calculations are not consistent with the results obtained in the previous studies and are only meant to indicate the possible range of σ^{res} . The upper curves for $c\bar{c}$ production are obtained with $m_c = 1.3 \text{ GeV}/c^2$, $\mu = m_c$ and the GRV HO densities while the lower curves are calculated with $m_c = 1.8 \text{ GeV}/c^2$, $\mu = 2m_c$ and the MRS D- $'$ densities. For $b\bar{b}$ production, the upper curves are calculated with $m_b = 4.5 \text{ GeV}/c^2$, $\mu = m_b/2$ and the GRV LO densities. The lower curves are obtained with $m_b = 5 \text{ GeV}/c^2$, $\mu = 2m_b$ and the GRV HO densities. (Since $\mu > Q_0$ for the GRV HO and MRS D- $'$ the same scales are used

⁶We note that if the MRS D- $'$ distributions were refit with a smaller Q_0 so that $\mu = m_c$ could be used, we would then expect the charm results to be similar to those with the GRV HO distributions.

in each, producing very similar results.) In Table 1 we show the appropriate value of α_s for each parton density and scale used to calculate both our central results and our extreme cases. To illustrate how the resummation technique works at the extremes, in Figs. 4 and 5 we compare σ^{res} and σ^{app} for the upper and lower bounds given by the dotted curves in Fig. 3.

In Fig. 4, the upper limit of $c\bar{c}$ production obtained using the GRV HO distributions produces convergence for $\mu_0 = 0.25m_c$ in the $q\bar{q}$ channel and $\mu_0 = 0.35m_c$ in the gg channel. These values, with $m_c = 1.3 \text{ GeV}/c^2$ are not so different from those we found with $m_c = 1.5 \text{ GeV}/c^2$. The smaller quark mass produces a stronger increase of σ^{res} with energy, as suggested in Fig. 3. The $\pi p \rightarrow c\bar{c}$ cross section already diverges at $\sqrt{S} = 15 \text{ GeV}$ in Fig. 3(a). The upper limit of $b\bar{b}$ production, calculated with the GRV LO distributions, converges for $\mu_0 = 0.11m_b$ in the $q\bar{q}$ channel and $0.15m_b$ in the gg channel. Note that the smaller scale, $m_b/2$, used for GRV LO results in a smaller μ_0 needed for resummation. However the variation of both σ^{res} and σ^{app} with μ_0 is quite strong since at $\mu_0 \approx 0.6m_b$, $s_0/m^2 \approx 1$ and the separation of the s_4 integral is no longer applicable. In this case, the $b\bar{b}$ cross section begins to diverge at large \sqrt{S} , due also in part to the large value of α_s for the lower scale.

In Fig. 5, the lower limit of $c\bar{c}$ production obtained using the MRS D—' distributions produces a convergent result for $\mu_0 = 0.5m_c$ in the $q\bar{q}$ channel and $\mu_0 = 0.7m_c$ in the gg channel. The larger value of m_c makes the resummation stable at higher energies. However, the resulting $K_{\text{exp}}^{\text{res}}$ is so large this possibility appears to be ruled out. The lower limit of $b\bar{b}$ production, calculated with the GRV HO distributions, converges for $\mu_0 = 0.425m_b$ in the $q\bar{q}$ channel and $0.625m_b$ in the gg channel. The ratio μ_0/m is similar for the lower limits of $c\bar{c}$ production since the scale is $\mu = 2m$ in both cases even though different parton densities were used. In general, it is the value of the scale that determines the μ_0 at which the resummed and approximate results converge rather than the quark mass. For example, in $b\bar{b}$ production in pp interactions, the MRS D—' and GRV HO distributions give similar results for μ_0 since $\mu = m_b$ can be used for both [23]. Note that the higher mass and scale increases the relative $q\bar{q}$ contribution, particularly for π^-p interactions.

To summarize, we have presented a comparison of the NLO and resummed cross sections for charm and bottom production using similar μ_0 values to those obtained for top quark production. The resummation of the S+V

logarithms produces an enhancement of the NLO results. The resummation technique appears to work reasonably well for $m_c = 1.5 \text{ GeV}/c^2$ and $m_b = 4.75 \text{ GeV}/c^2$, resulting also in $K_{\text{exp}}^{\text{res}} \approx 1$. At the moment, for a consistent description of both $c\bar{c}$ and $b\bar{b}$ production by pions and protons, the GRV HO distributions are the only choice available. We reach this conclusion concerning the GRV HO densities for two reasons: It is currently the only set with the same low x treatment of the pion and proton parton distribution functions. It also allows us to treat the scale on the same level for all heavy quarks, $\mu = m_Q$, producing a uniform convergence of the resummed cross sections at the same μ_0 for charm, bottom, and top. Presumably another set of parton distributions that satisfies these criteria would produce results similar to those given in Fig. 2 and the central curves of Fig. 3. More precise data on the charm, bottom and top production cross sections in the threshold regions should clarify the situation and yield interesting information on the interplay between perturbative and nonperturbative physics.

Acknowledgements The work in this paper was supported in part under the contract NSF 93-09888.

References

- [1] S.P.K. Tavernier, Rep. Prog. Phys. 50 (1987) 1439. This review contains references to all data prior to 1988, including the ISR measurements.
- [2] J.A. Appel, Ann. Rev. Nucl. Part. Science 42 (1992) 367.
- [3] P. Nason, S. Dawson, and R.K. Ellis, Nucl. Phys. B303 (1988) 607.
- [4] W. Beenakker, H. Kuijf, W.L. van Neerven, and J. Smith, Phys. Rev. D40 (1989) 54.
- [5] W. Beenakker, W.L. van Neerven, R. Meng, G.A. Schuler, and J. Smith, Nucl. Phys. B351 (1991) 507.
- [6] J.C. Collins, D.E. Soper and G. Sterman, *in* Perturbative QCD, ed. A.H. Mueller (World Scientific, Singapore, 1989).
- [7] P.L. McGaughey *et al.*, Int. J. Mod. Phys. A10 (1995) 2999.

- [8] R. Vogt, Z. Phys. C71 (1996) 475.
- [9] S. Frixione, M.L. Mangano, P. Nason, and G. Ridolfi, Nucl. Phys. B431 (1994) 453.
- [10] K. Kodama *et al.*, E653 Collab., Phys. Lett. B263 (1991) 573; M. Aguilar-Benitez *et al.*, LEBC-EHS Collab., Z. Phys. C40 (1988) 321; S. Barlag *et al.*, ACCMOR Collab., Z. Phys. C39 (1988) 451.
- [11] M. Sarmiento *et al.*, E515 Collab., Phys. Rev. D45 (1992) 2244; S. Barlag *et al.*, ACCMOR Collab., Z. Phys. C49 (1991) 555; G.A. Alves *et al.*, E769 Collab., Phys. Rev. Lett. 69 (1992) 3147; K. Kodama *et al.*, E653 Collab., Phys. Lett. B284 (1992) 461.
- [12] H. Plochow-Besch, Comp. Phys. Comm. 75 (1993) 396.
- [13] P.J. Sutton, A.D. Martin, R.G. Roberts, and W.J. Stirling, Phys. Rev. D45 (1992) 2349.
- [14] A.D. Martin, R.G. Roberts, and W.J. Stirling, Phys. Lett. B306 (1993) 145.
- [15] M. Glück, E. Reya, and A. Vogt, Z. Phys. C53 (1992) 651.
- [16] M. Glück, E. Reya, and A. Vogt, Z. Phys. C53 (1992) 127.
- [17] E. Laenen, J. Smith, and W.L. van Neerven, Nucl. Phys. B369 (1992) 543.
- [18] G. Sterman, Nucl. Phys. B281 (1987) 310. More recent references can be located by consulting L. Alvero and H. Contopanagos, Nucl. Phys. B436 (1995) 184; ITP-SB-94-41 (1995); P.J. Rijken and W.L. van Neerven, Phys. Rev. D51 (1995) 44.
- [19] S. Catani and L. Trentadue, Nucl. Phys. B327 (1989) 323; B353 (1991) 183.
- [20] E. Laenen, J. Smith, and W.L. van Neerven, Phys. Lett. B321 (1994) 254.
- [21] N. Kidonakis and J. Smith, Phys. Rev. D51 (1995) 6092.

- [22] D. Appel, P. Mackenzie and G. Sterman, Nucl. Phys. B309 (1988) 259.
- [23] N. Kidonakis and J. Smith, Mod. Phys. Lett. A11 (1996) 587.
- [24] H. Aubrecht *et al.*, Letter of Intent, DESY-PRC 92/04 (1992).
- [25] H. Aubrecht *et al.*, Progress Report, DESY-PRC 93/04 (1993).
- [26] E.L. Berger and H. Contopanagos, Phys. Lett. B361 (1995) 115; hep-ph/9603326, March 1996.
- [27] P. Bordalo *et al.*, NA10 Collab., Z. Phys. C39 (1988) 7; K. Kodama *et al.*, E653 Collab., Phys. Lett. B303 (1993) 359; M.G. Catanesi *et al.*, WA78 Collab., Phys. Lett. B231 (1989) 328; R. Jesik *et al.*, E672-E706 Collab., Phys. Rev. Lett. 74 (1995) 495.

$c\bar{c}$			
	GRV HO (2 loop)	GRV HO (2 loop)	MRS D- $'$ (2 loop)
Λ_3 (MeV/ c)	248	248	280
m_c (GeV/ c^2)	1.3	1.5	1.8
μ/m_c	1	1	2
α_s	0.3	0.278	0.204
$b\bar{b}$			
	GRV LO (1 loop)	GRV HO (2 loop)	GRV HO (2 loop)
Λ_4 (MeV/ c)	200	200	200
m_b (GeV/ c^2)	4.5	4.75	5.0
μ/m_b	0.5	1	2
α_s	0.312	0.187	0.155

Table 1: The values of Λ_f and α_s for each of the parton densities and scales we consider. The left column gives the parameters for the upper bound on σ^{res} . The middle column shows the parameters used for our principle results. The right column displays the parameters that give the lower bound on σ^{res} .

Figure Captions

Fig. 1. Fractional contributions of the NLO channels to the total $O(\alpha_s^3)$ $c\bar{c}$ and $b\bar{b}$ production cross sections as functions of \sqrt{S} . We use $m_c = 1.5$ GeV/ c^2 , $m_b = 4.75$ GeV/ c^2 , and the GRV HO parton densities with the two-loop corrected α_s from PDFLIB [12]. All the contributions are given in the $\overline{\text{MS}}$ scheme. We show the gg (solid), $q\bar{q}$ (dashed), and $(q + \bar{q})g$ (dot-dashed), contributions to $c\bar{c}$ production in (a) π^-p interactions and (b) pp interactions and $b\bar{b}$ production in (c) π^-p and (d) pp interactions.

Fig. 2. The μ_0 dependence of the resummed cross section for $c\bar{c}$ and $b\bar{b}$ production. We use $m_c = 1.5$ GeV/ c^2 , $m_b = 4.75$ GeV/ c^2 , and the GRV HO parton densities with the uncorrected two-loop α_s . All the contributions are given in the $\overline{\text{MS}}$ scheme. We show $\sigma_{q\bar{q}}^{\text{res}}$ (solid), σ_{gg}^{res} (dashed), $\sigma_{q\bar{q}}^{\text{app}}$ (dot-dashed) and σ_{gg}^{app} (dotted) at $\sqrt{S} = 15$ GeV for $c\bar{c}$ production in (a) π^-p and (b) pp interactions and at $\sqrt{S} = 30$ GeV for $b\bar{b}$ production in (c) π^-p and (d) pp interactions.

Fig. 3. The resummed, improved, and NLO cross sections are shown as functions of \sqrt{S} for the $c\bar{c}$ and $b\bar{b}$ production. We show the total resummed cross section (solid) and the total improved cross section (dashed), both with $\mu_0 = 0.15m$ for the $q\bar{q}$ channel and $\mu_0 = 0.35m$ for the gg channel, and the total $O(\alpha_s^3)$ cross section (dot-dashed) results with $\mu = m$ using $m_c = 1.5$ GeV/ c^2 and $m_b = 4.75$ GeV/ c^2 . We also show the extreme values of σ^{res} obtained when varying the quark mass, scale, and parton densities in the dotted lines. The results are given for $c\bar{c}$ production in (a) π^-p interactions and (b) pp interactions and $b\bar{b}$ production in (c) π^-p and (d) pp interactions.

Fig. 4. The μ_0 dependence of the upper bound of the resummed $c\bar{c}$ and $b\bar{b}$ production cross sections shown in the upper dotted curves of Fig. 3. We show $\sigma_{q\bar{q}}^{\text{res}}$ (solid), σ_{gg}^{res} (dashed), $\sigma_{q\bar{q}}^{\text{app}}$ (dot-dashed) and σ_{gg}^{app} (dotted) at $\sqrt{S} = 15$ GeV for $c\bar{c}$ production in (a) π^-p and (b) pp interactions and at $\sqrt{S} = 30$ GeV for $b\bar{b}$ production in (c) π^-p and (d) pp interactions. For $c\bar{c}$ production, the curves correspond to the upper dotted curves in Fig. 3(a) and (b) with $\mu = m_c = 1.3$ GeV/ c^2 and the GRV HO densities. For $b\bar{b}$ pro-

duction, the curves correspond to the upper dotted curves in Fig. 3(c) and (d) with $2\mu = m_b = 4.5 \text{ GeV}/c^2$ and the GRV LO densities.

Fig. 5. The μ_0 dependence of the lower bound of the resummed $c\bar{c}$ and $b\bar{b}$ production cross sections shown in the lower dotted curves of Fig. 3. We show $\sigma_{q\bar{q}}^{\text{res}}$ (solid), σ_{gg}^{res} (dashed), $\sigma_{q\bar{q}}^{\text{app}}$ (dot-dashed) and σ_{gg}^{app} (dotted) at $\sqrt{S} = 15 \text{ GeV}$ for $c\bar{c}$ production in (a) π^-p and (b) pp interactions and at $\sqrt{S} = 30 \text{ GeV}$ for $b\bar{b}$ production in (c) π^-p and (d) pp interactions. For $c\bar{c}$ production, the curves correspond to the lower dotted curves in Fig. 3(a) and (b) with $\mu/2 = m_c = 1.8 \text{ GeV}/c^2$ and the MRS D- $'$ densities. For $b\bar{b}$ production, the curves correspond to the lower dotted curves in Fig. 3(c) and (d) with $\mu/2 = m_b = 5 \text{ GeV}/c^2$ and the GRV HO densities.

Figure 1

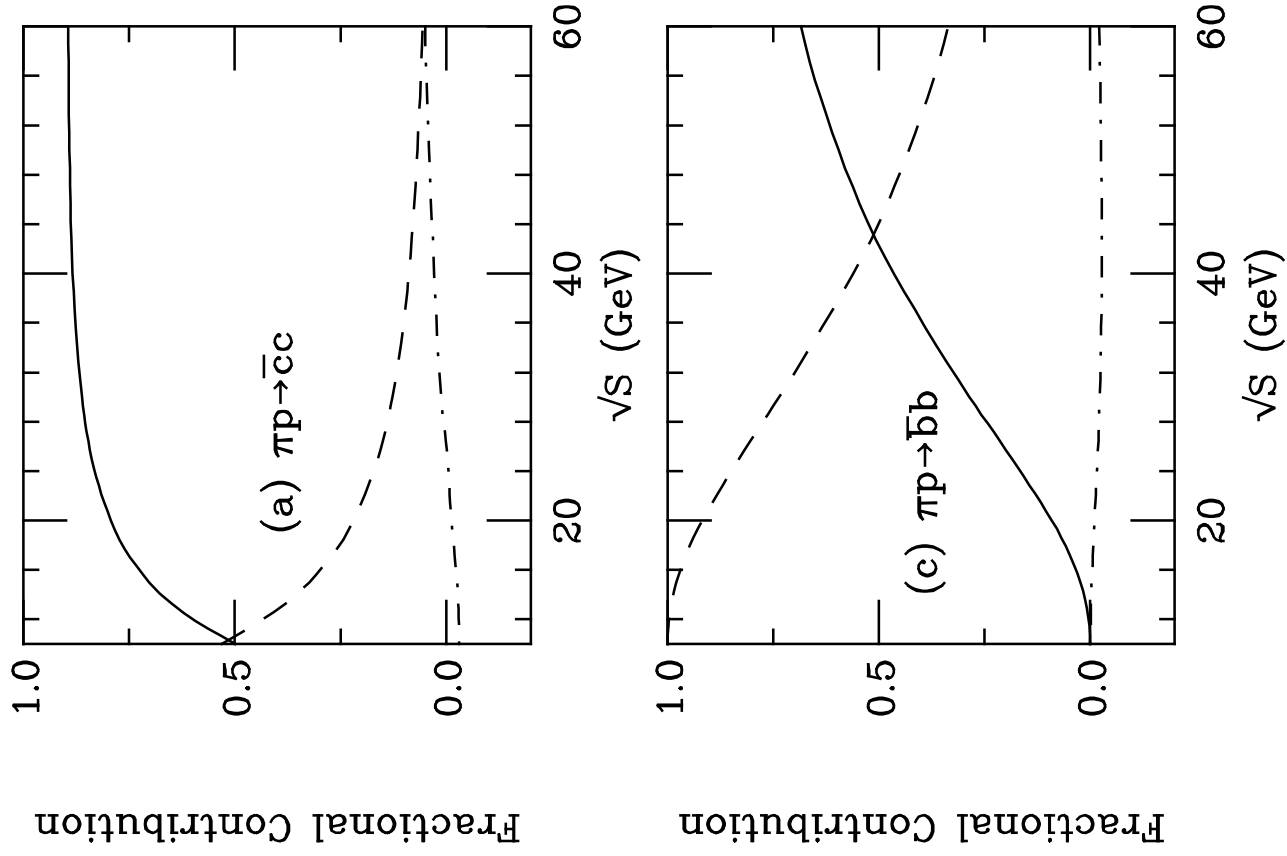


Figure 2

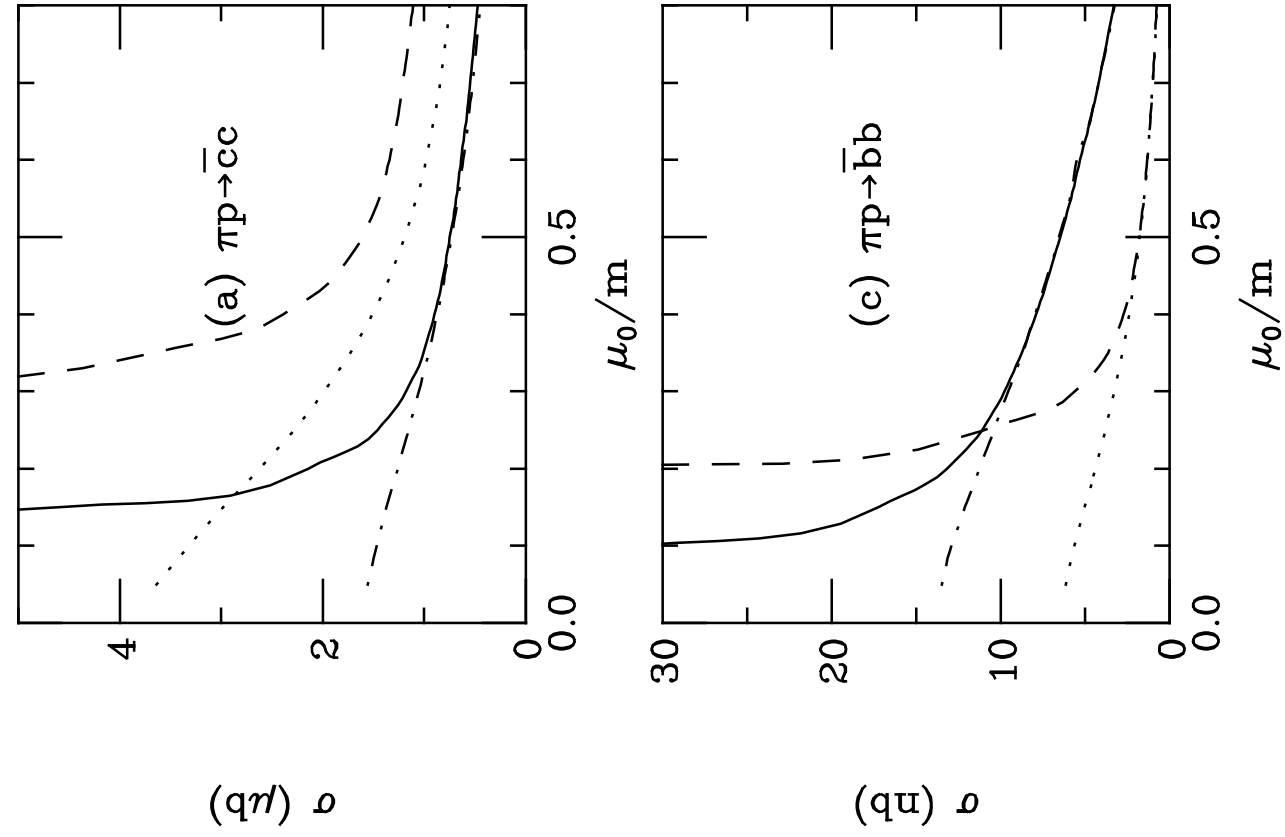


Figure 3

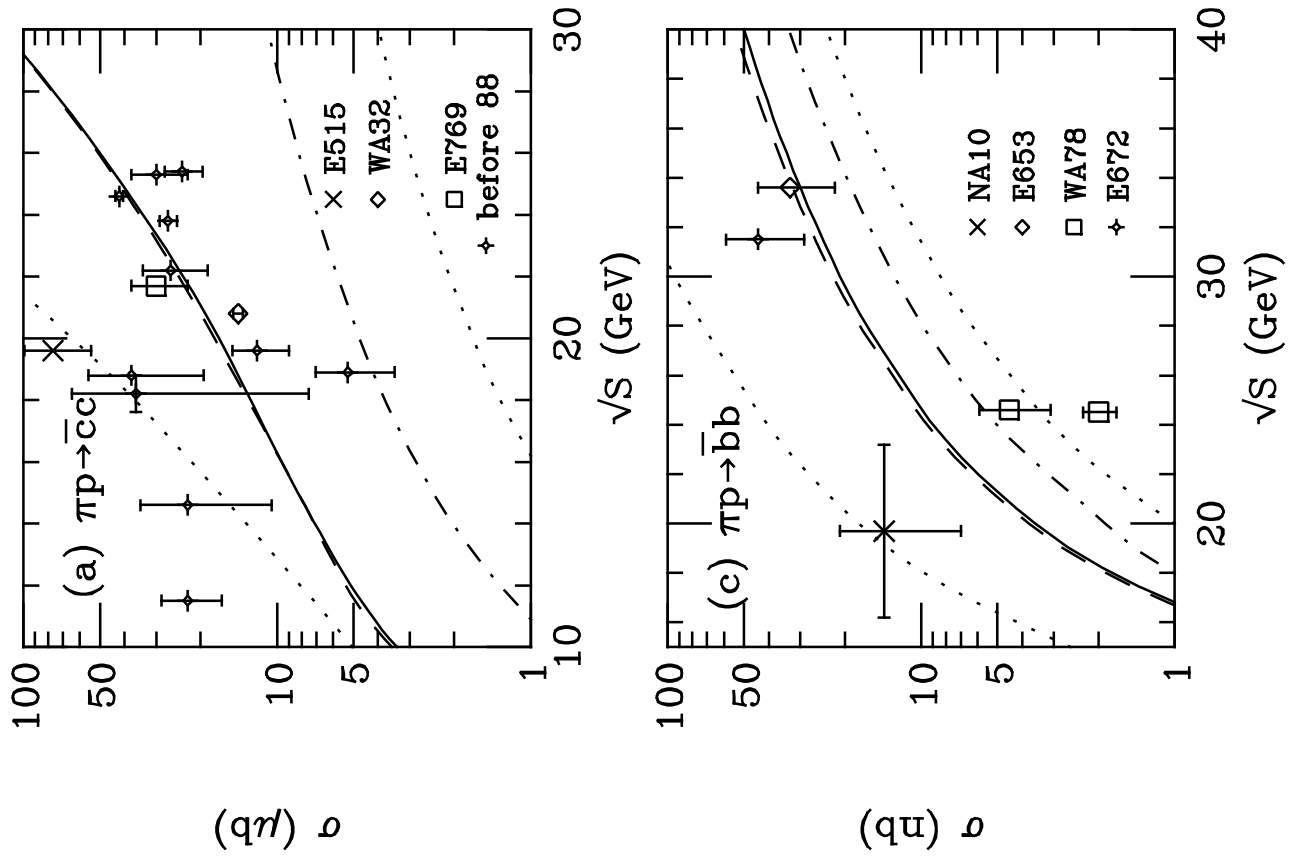


Figure 4

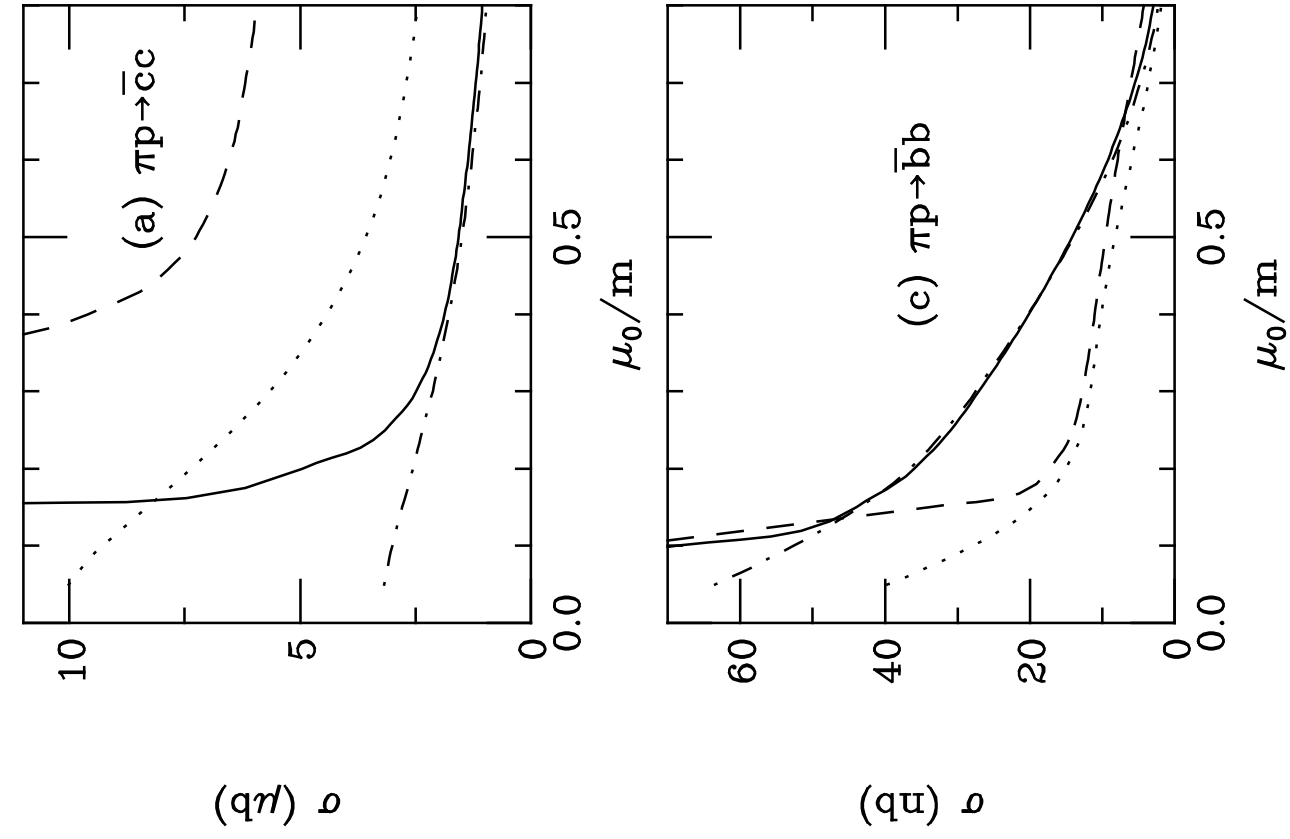


Figure 5

